We are IntechOpen,
the world's leading publisher of
Open Access books
Built by scientists, for scientists

6,900
Open access books available

185,000
International authors and editors

200M
Downloads

154
Countries delivered to

Our authors are among the

TOP 1%
most cited scientists

12.2%
Contributors from top 500 universities

CLARIVATE ANALYTICS
BOOK CITATION INDEX INDEXED

WEB OF SCIENCE™

Selection of our books indexed in the Book Citation Index
in Web of Science™ Core Collection (BKCI)

Interested in publishing with us?
Contact book.department@intechopen.com

Numbers displayed above are based on latest data collected.
For more information visit www.intechopen.com

Formation of Cuspate Foreland

Takaaki Uda, Masumi Serizawa and Shiho Miyahara

Abstract

The formation of a cuspate foreland when waves were incident from two opposite directions was investigated, taking a cuspate foreland extending at the northeast end of Graham Island in British Colombia of Canada and the cuspate forelands formed at the tip of Hon Bip Island north of Nha Trang, Vietnam, as the examples. The formation of such a cuspate foreland was predicted using the Type 4 BG model. Then, the development of multiple sand spits with rhythmic shapes in a shallow water body was investigated, taking the Sea of Azov in Russia as the example. Furthermore, the development of sand spits and cuspate forelands with rhythmic shapes was predicted, assuming that the waves were obliquely incident at angles of 60° relative to the direction normal to the shoreline or at angles of ±60° with probability $p_1:p_2$ = 0.50:0.50, 0.60:0.40, 0.65:0.35, 0.70:0.30, 0.75:0.25, and 0.80:0.20.

Keywords: cuspate foreland, sand spits, Sea of Azov, Graham Island, Hon Bip Island, rhythmic shapes, shoreline instability, wave-sheltering effect

1. Introduction

A sand spit is a dynamically changing topography formed by the successive deposition of littoral sand when waves are obliquely incident at a large angle relative to the direction normal to the shoreline [1, 2]. A cuspate foreland is another topography protruding into the sea, and it could be formed when waves are incident from two opposite directions, and a cuspate foreland of symmetric or asymmetric shape could be formed depending on the probability of the occurrence of incident waves. Ashton et al. [2] and Ashton and Murray [3] developed a model for predicting the formation of cuspate forelands with rhythmic shapes when waves were obliquely incident from two opposite directions at an angle greater than approximately 45° relative to the direction normal to the shoreline. The present authors also proposed a model for predicting the topographic changes of cuspate forelands with rhythmic shapes using the BG model [4, 5]. However, there were no studies on the formation of a cuspate foreland when waves were incident from two completely opposite directions. Therefore, the morphological characteristics of the cuspate foreland located at the northeast end of Graham Island in British Colombia of Canada and the cuspate forelands formed at the tip of Hon Bip Island north of Nha Trang, Vietnam, were investigated, and then the development of a cuspate foreland when waves were obliquely incident from two opposite directions was predicted using the Type 4 BG model in Section 2 [6].

Zenkovich [1] showed that multiple sand spits with rhythmic shapes may develop in shallow bodies of water, such as the Azov Sea, and called them the Azov-type spits. **Figure 1** shows the satellite image of multiple sand spits with rhythmic shapes developed in t17, the Azov Sea in Russia, and an enlarged image
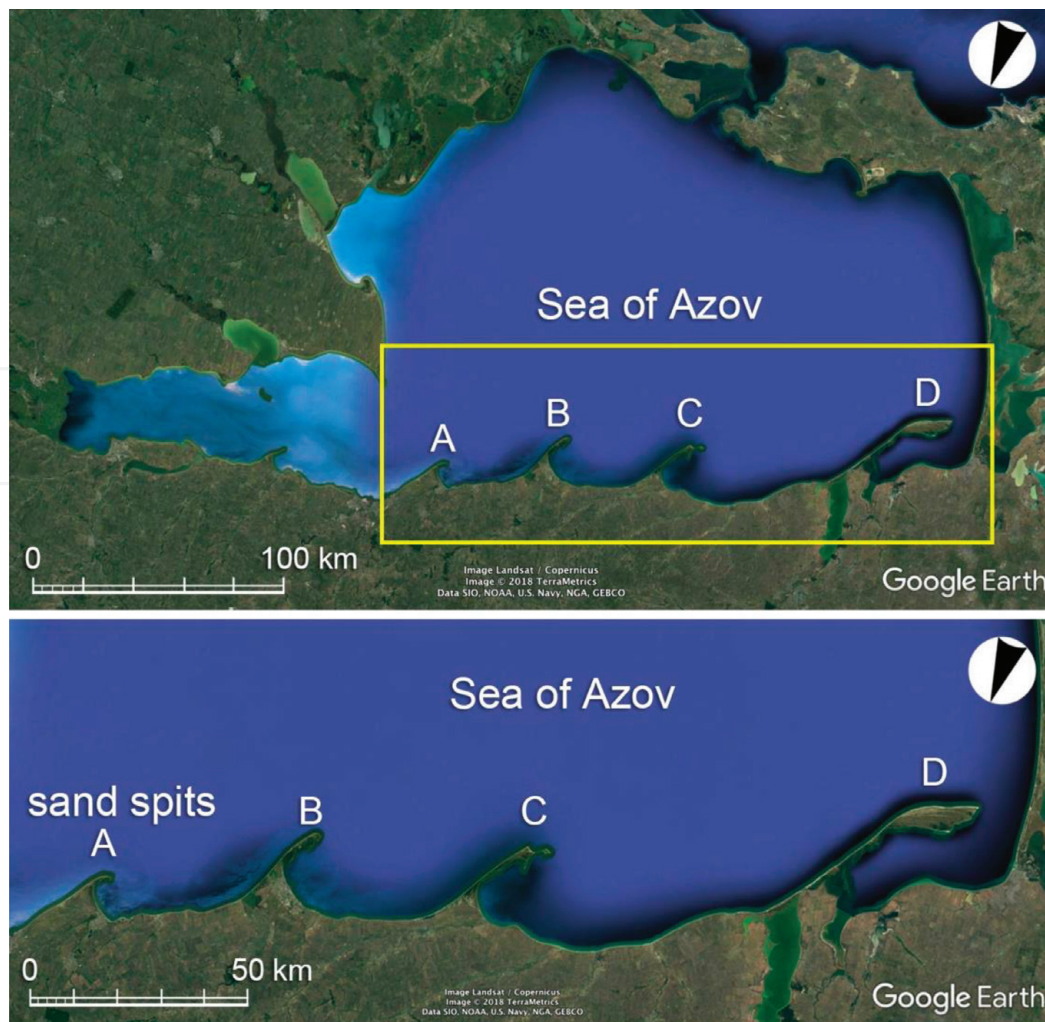
Figure 1.
Multiple sand spits with rhythmic shapes developed in Sea of Azov in Russia [5].

of the rectangular area in **Figure 1**. He concluded that shoreline instability may occur when waves are obliquely incident at an angle larger than 45°, and the wave-sheltering effect due to the sand spits themselves plays an important role in the development of sand spits. Ashton et al. [2] adopted this mechanism and successfully modeled the shoreline instability, and this mechanism was called high-angle wave instability [3]. Littlewood et al. [7] predicted the shoreline of log-spiral bays using their model. In Section 3, we predicted the development of sand spits and cuspate forelands when waves were obliquely incident at an angle larger than 45°, given a small perturbation in the initial topography, and showed that the three-dimensional (3-D) beach changes of sand spits and cuspate forelands with rhythmic shapes can be predicted using the Type 4 BG model [4, 5]. van den Berg et al. [8] predicted the development of sand waves caused by high-angle wave instability using equations similar to that of our model, but not the development of sand spits or cuspate forelands.

2. Model for predicting formation of a cuspate foreland

2.1 Cuspate foreland extending at northeast end of Graham Island

A large cuspate foreland extends at the northeast end of Graham Island in British Colombia of Canada, as shown in **Figure 2** [6, 9]. Graham Island is located north of Moresby Island with a narrow channel separating these islands. The

coastlines of these islands face the Pacific Ocean to the west and extend for 300 km in the SE-NW direction. At the north end of Graham Island, Dixon Entrance of 46 km width is located, and the cuspate foreland extends east of the entrance along with Hecate Strait on the south side. The primary and secondary wave directions are from NW and SSE, respectively, from these geometrical conditions [6].
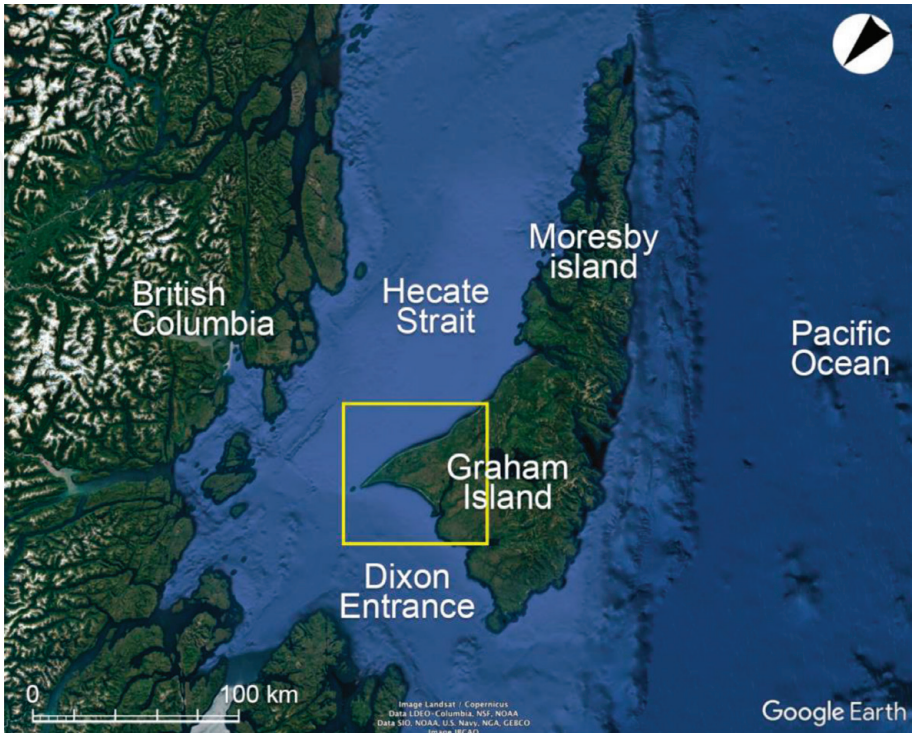

Figure 2.
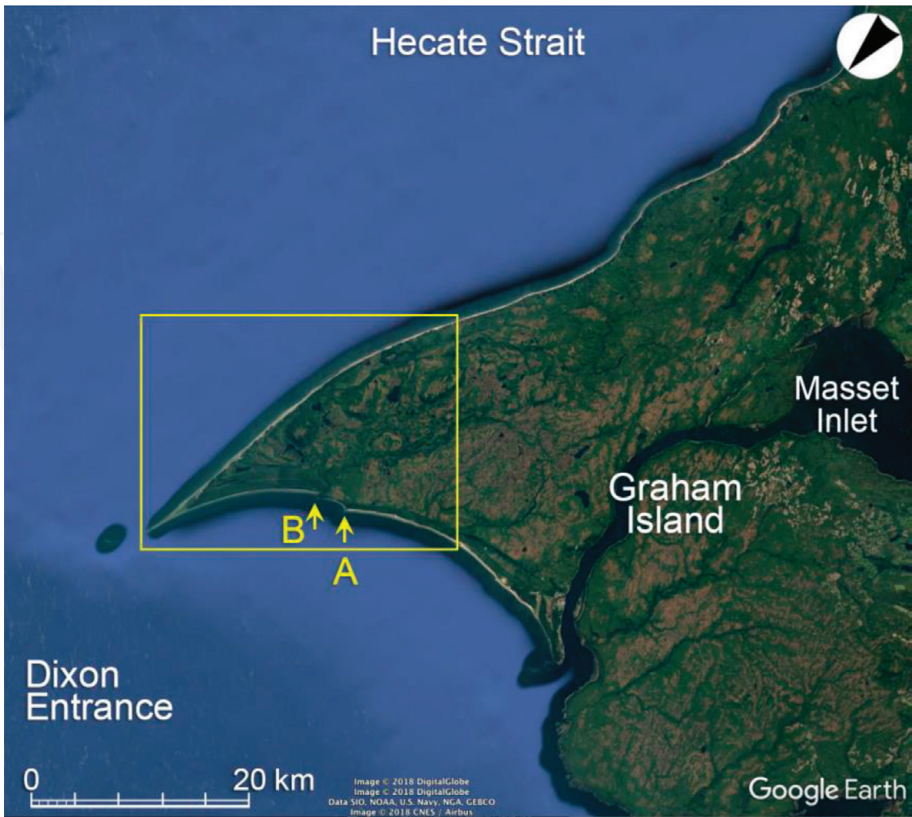*Location of cuspate foreland at northeast end of Graham Island in Canada.*

Figure 3.
*Enlarged satellite image of cuspate foreland (rectangular area in **Figure 2**).*

Figure 4.
*Enlarged satellite image of sand ridges and a closed water body C (rectangular area in **Figure 3**).*

Figure 3 shows an enlarged satellite image of the rectangular area in **Figure 2**; the entire coastline west of the foreland has a concave shape, and a hooked shoreline is formed east of points A and B. This means that longshore sand transport toward the tip of the cuspate foreland prevails because of the waves incident from the Pacific Ocean via Dixon Entrance located northwest of the foreland. Furthermore, a number of beach ridges run in parallel with the present shoreline east of point B, as shown in **Figure 4**, which is an enlarged satellite image of the rectangular area in **Figure 3**, implying that sand transported northeastward was deposited to form the cuspate foreland. In contrast, no beach ridges develop along the east coastline extending in the S–N direction, and a number of sand dunes have been formed by the SE wind at an angle of 40° relative to the direction normal to the mean coastline [6]. The development of these sand dunes clearly demonstrates that the coast along the eastern side of the foreland is subjected to the action of the wind waves incident from SE, resulting in the predominance of northward longshore sand transport toward the tip of the foreland. All these conditions of longshore sand transport promote the development
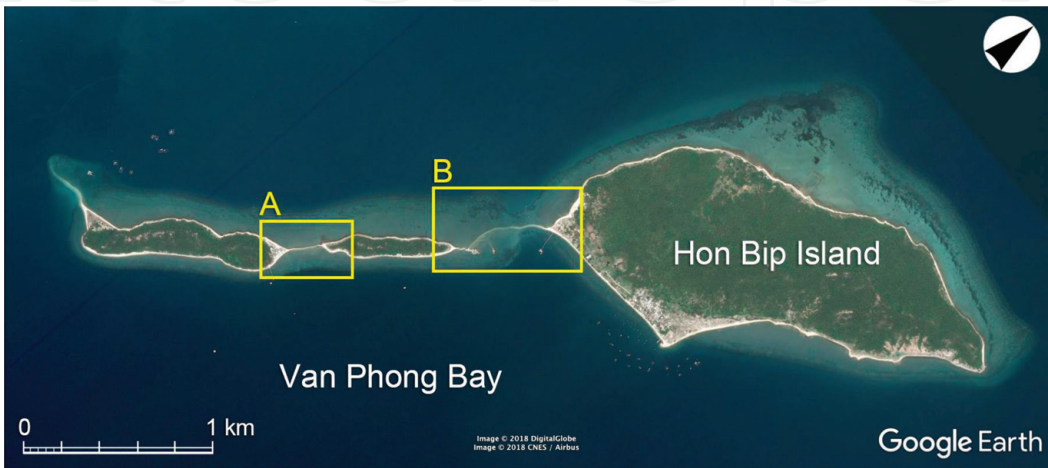

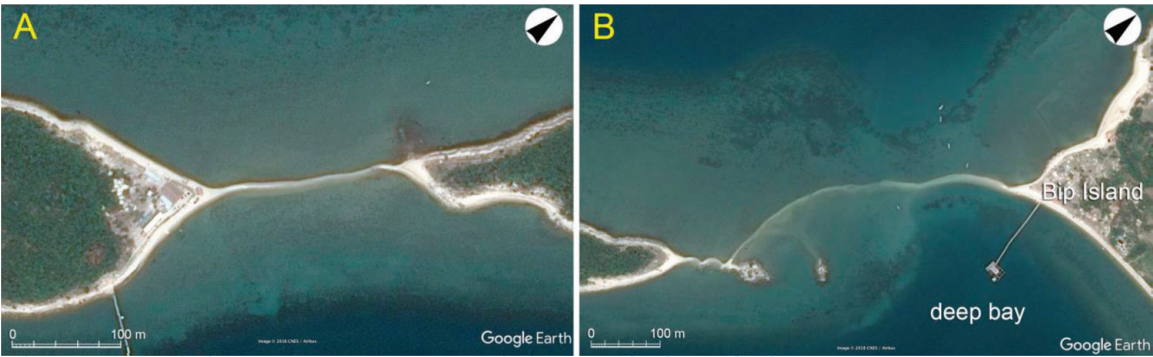**Figure 5.**
Hon Bip Island in Van Phong Bay in Vietnam.

Figure 6.
*Enlarged satellite images of areas A and B in **Figure 5**.*

of the cuspate foreland. Moreover, water bodies enclosed inland of the cuspate foreland can be seen near point C in **Figure 4**, which is assumed to be closely related to the formative mechanism of a cuspate foreland.

2.2 Land-tied islands and cuspate foreland on Hon Bip Island

Hon Bip Island is located in Van Phong Bay north of Nha Trang, Vietnam. In the vicinity of this island, a land-tied island and a cuspate foreland are formed [10], similarly to the cases on Yoshima Island offshore of Shodo Island [11]. **Figure 5** shows a satellite image of Hon Bip Island. A shallow sea extends on the southwest
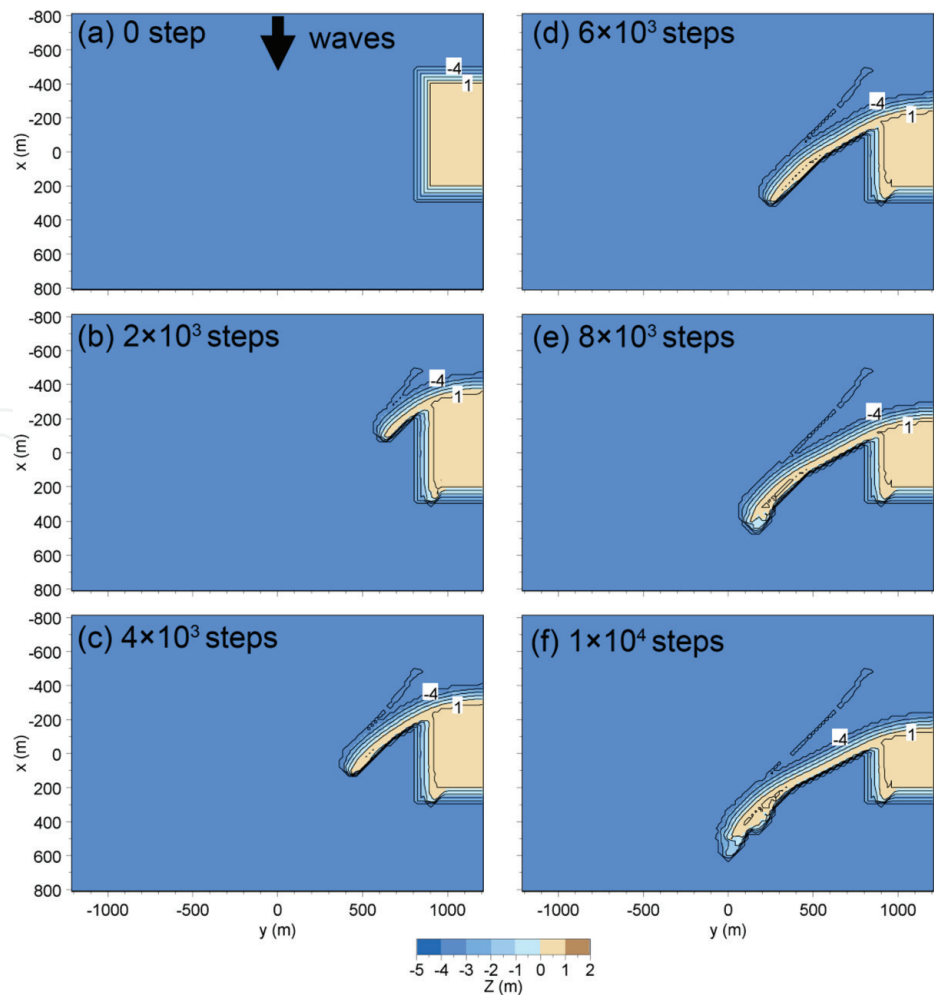

Figure 7.
Extension of single sand spit in Case 1.

side of this island, and slender islands of 0.7 and 1.07 km lengths exist, and sand bars of 0.53 and 0.20 km lengths connecting the islands extend to form a land-tied island. Furthermore, from the southwest end of the islands, a small-scale cuspate foreland extends westward. **Figure 6** shows the enlarged satellite images of areas A and B, shown in **Figure 5**. The cuspate foreland extends straight in a shallow sea between the islands in area A. In contrast, a deep bay approaches the cuspate foreland from the east in area B, resulting in the formation of a bay-shaped shoreline on the east side of the cuspate foreland. Thus, the cuspate foreland can extend in the shallow sea between the islands owing the wave-sheltering effect of the islands.

2.3 Calculation conditions

To predict the formation and deformation of a cuspate foreland, the Cartesian coordinates of (x, y) were introduced, and a rectangular area of 2.4 km width and 1.6 km length was adopted as the calculation domain (**Figure 7(a)**). The water depth was assumed to be a constant of 4 m, and a sandy beach with 1 m height and 1/20 slope was set along the rectangular shoreline as the initial condition. The incident wave height was assumed to be 1 m. Four cases of calculation were carried out; a single wave from the $-x$-axis in Case 1, waves with the equivalent probability of 0.5 incident from two opposite directions in Case 2, and waves incident from two opposite directions with the probabilities of $p_1 = 0.75$ from the $-x$-axis (downward) and $p_2 = 0.25$ from the $+x$-axis (upward) in Case 3. In addition, in Case 4, the

Calculation method	Type 4 BG model
Wave conditions	Incident waves: $H_I = 1$ m, $T = 4$ s, wave direction $\theta_I = 0°$, and 180° relative to x-axis
Berm height	$h_R = 1$ m
Depth of closure	$h_c = 4$ m
Equilibrium slope	$\tan\beta_c = 1/20$
Angle of repose slope	$\tan\phi = 1/2$
Coefficients of sand transport	Coefficient of longshore sand transport $K_s = 0.2$ Coefficient of Ozasa and Brampton [12] term $K_2 = 1.62K_s$ Coefficient of cross-shore sand transport $K_n = K_s$
Mesh size	$\Delta x = \Delta y = 20$ m
Time intervals	$\Delta t = 0.5$ h
Duration of calculation	10^4 h (2×10^4 steps)
Boundary conditions	Shoreward and landward ends, $q_x = 0$; right and left boundaries, $q_y = 0$
Calculation of wave field	Energy balance equation [13]
	• Term of wave dissipation due to wave breaking: Dally et al. [14] model
	• Wave spectrum of incident waves: directional wave spectrum density obtained by Goda [15]
	• Total number of frequency components $N_F = 1$ and number of directional subdivisions $N_\theta = 8$
	• Directional spreading parameter $S_{max} = 25$
	• Coefficient of wave breaking $K = 0.17$ and $\Gamma = 0.3$
	• Imaginary depth between minimum depth h_0 (0.5 m) and berm height h_R
	• Wave energy = 0 where $Z \geq h_R$
	• Lower limit of h in terms of wave decay due to breaking, 0.5 m

Table 1.
Conditions for calculation of formation of a cuspate foreland.

extension of cuspate forelands, their connection and merging in a shallow water body between two islands were numerically simulated. The wave direction was determined using random numbers when waves were incident from two opposite directions. **Table 1** summarizes the conditions for the calculation of the formation of a cuspate foreland.

2.4 Calculation results

First, the formation of a single sand spit in Case 1 is shown in **Figure 7** in which a single wave was incident from the $-x$-axis. The beach on the exposed side was eroded, and sand was transported obliquely by longshore sand transport, and a single sand spit extended (**Figure 7(b)–(f)**). As the sand spit extended, a wave-shelter zone was formed behind the sand spit itself, so that no beach changes occurred behind the sand spit except the downdrift corner of the initial rectangular sandy island.

When waves were incident from two completely opposite directions with the same probability, as in Case 2, sand spits were soon formed at the right corners of the rectangular sand mound (**Figure 8(b)**) [6]. Then, the sand spits that independently
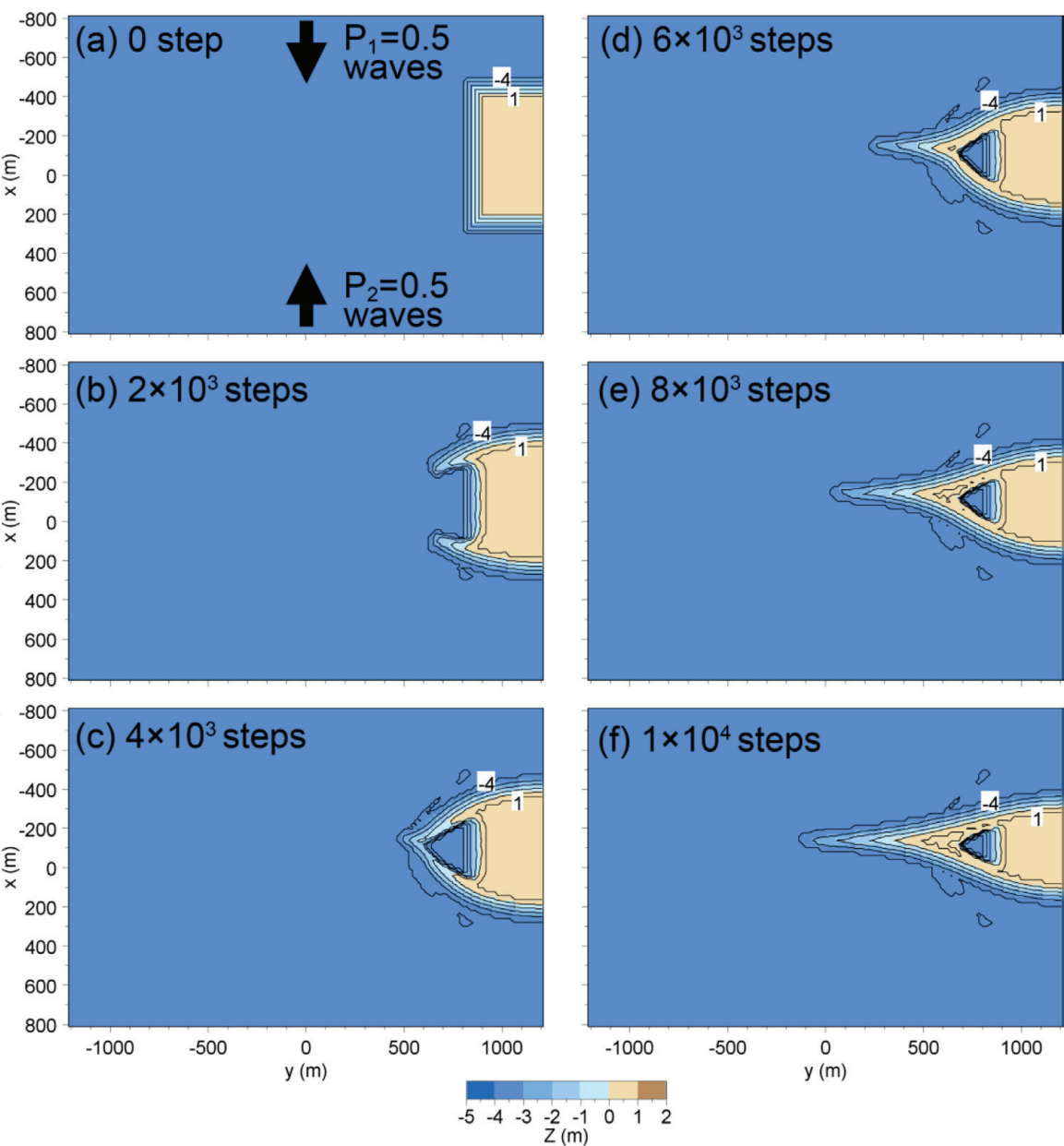

Figure 8.
Extension of cuspate foreland in Case 2.

developed at each corner were pulled to each other and connected because of the wave-sheltering effect of a sand spit at one side to the other (**Figure 8(c)**). Finally, a triangular, completely closed water body was formed at the central part after 6×10^3 steps (**Figure 8(d)**). The size of the closed water body gradually decreased over time because of the deposition of sand owing to cross-shore sand transport, although the tip of the foreland continued to extend leftward, as shown in **Figure 8 (e** and **f)**. These results are in good agreement with the measured at the northeast end of
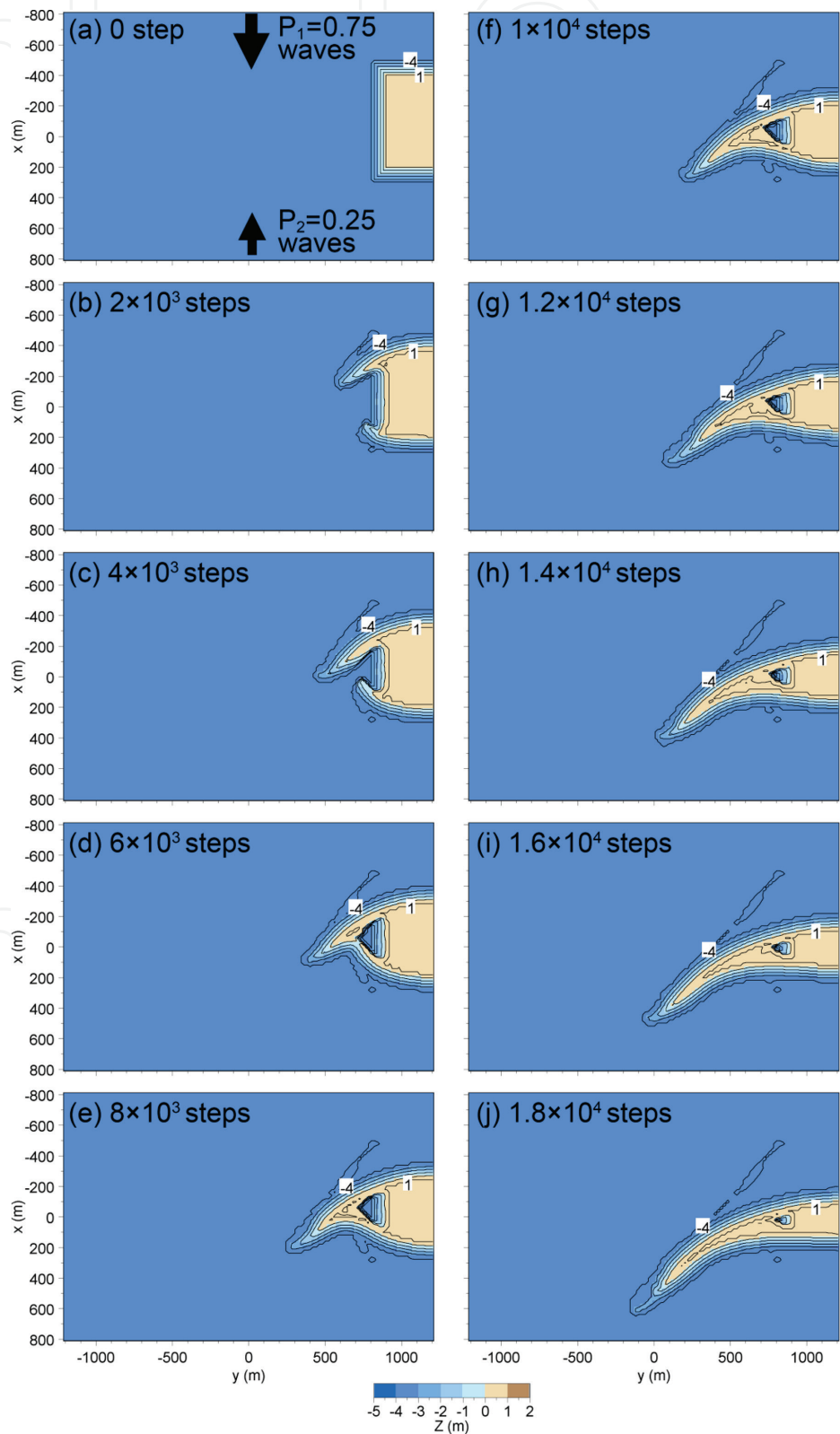

Figure 9.
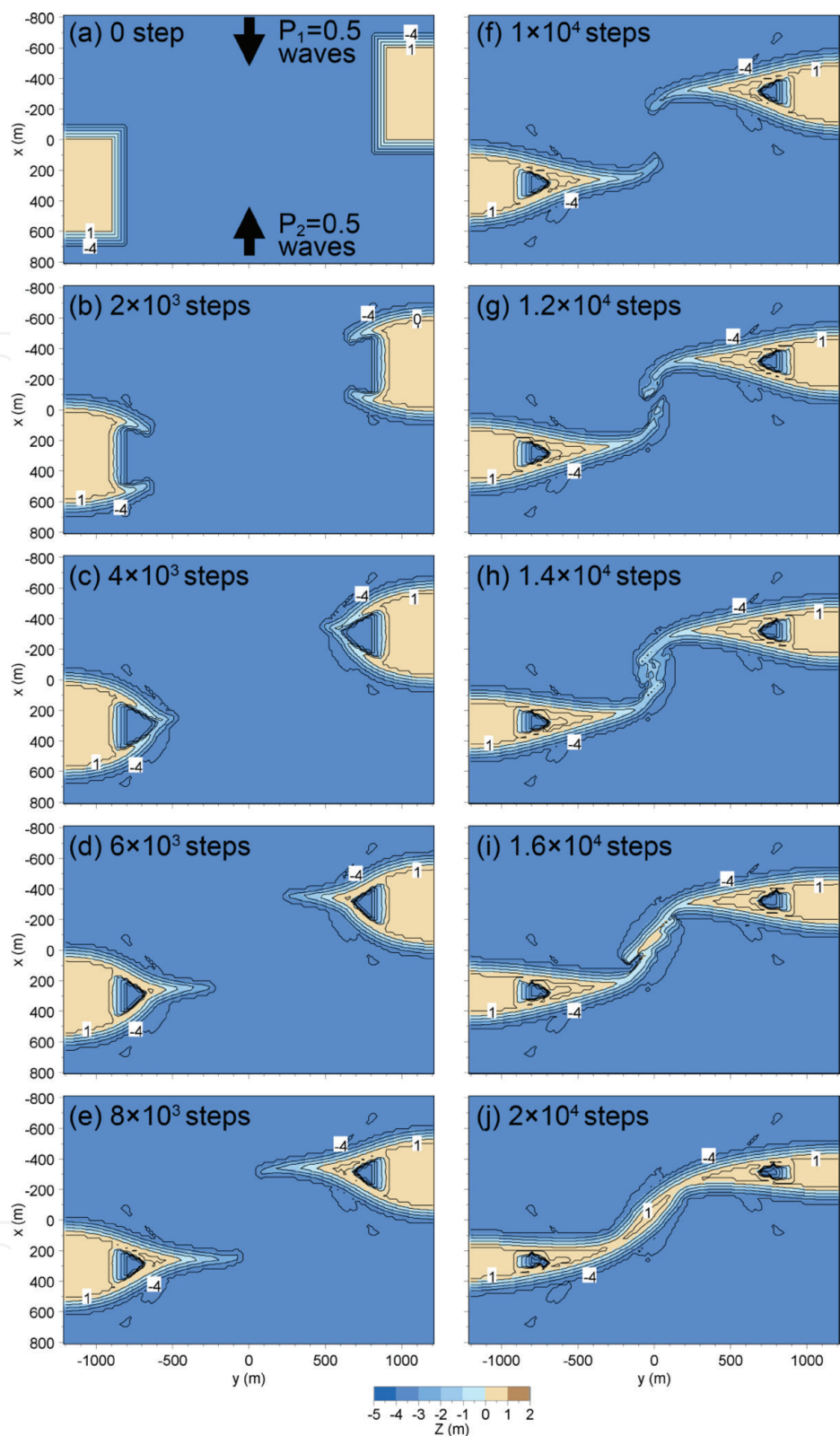*Extension of cuspate foreland in Case 3.*

Figure 10.
Extension, connection, and merging of two cuspate forelands (Case 4).

Graham Island in terms of the formation of a closed water body in the central part of the cuspate foreland, as shown in **Figure 4**.

When waves were incident from two opposite directions with different probabilities as in Case 3, an asymmetric cuspate foreland developed (**Figure 9**). At the initial stage, there existed a rectangular sand mound (**Figure 9(a)**). A cuspate foreland on the upper side elongated faster than that on the lower side because of a larger probability of waves, as shown in **Figure 9 (b** and **c)**, and a distorted closed water body was formed in the central part up to 6×10^3 steps (**Figure 9(d)**). Then, the cuspate

foreland further extended over time, and the size of this distorted closed water body decreased (**Figure 9(f)–(i)**). By 1.8×10^4 steps, a triangular closed water body was almost buried with sand with the recession of the upside shoreline, reducing the size (**Figure 9(j)**).

In Case 4, two sandy islands were set on both sides of the calculation domain, and waves were randomly incident from the $\pm x$-directions with the same probability of 0.5, as shown in **Figure 10**. The cuspate forelands started to elongate from both ends of the sandy islands toward the y-axis and became a flatter shape owing to the action of the waves incident from the $\pm x$-axis directions after 2000 steps (**Figure 10(b)**). Two triangular closed water bodies were formed on both sides up to 4×10^3 steps (**Figure 10(c)**). The cuspate forelands further developed after 6×10^3 steps (**Figure 10(d)**). After 8×10^3 steps, the tips of the slender cuspate forelands extending from the ends of the two islands had pulled each other, and their tips started to bend inward (**Figure 10(e)**). After 1.2×10^4 steps, cuspate forelands at the tips were about to connect (**Figure 10(g)**), and they were almost connected to each other after 1.4×10^4 steps, resembling shaking hands (**Figure 10(h)**). Then, the two islands were connected to each other, and a smooth shoreline was formed after 2×10^4 steps (**Figure 10(j)**).

3. Development of sand spits and cuspate forelands with rhythmic shapes

3.1 Calculation conditions

Ashton and Murray [3] showed that the generation of shoreline instability closely depended on the probability of occurrence of wave directions; sand spits, cuspate bumps, and sand spits with hooked shoreline developed in the case that the probability of occurrence of a unidirectional wave was high, the probability of occurrence of waves incident from two directions was equivalent, and waves were incident from two directions with different probabilities, respectively. The calculation conditions in this study were determined referring their results [4, 5]. As the wave conditions, $H_i = 1$ m and $T = 4$ s were assumed considering the formation of sand spits in a shallow lagoon. The wave direction was assumed to be obliquely incident at an angle of 60° and at angles of ±60° with probability $p_1:p_2 = 0.50:0.50$, 0.60:0.40, 0.65:0.35, 0.70:0.30, 0.75:0.25, and 0.80:0.20, and the wave direction at each step was determined from the probability distribution [4, 5].

Consider a shallow lake with a flat solid bed of 4 m depth, and the initial beach slope and a berm height assumed to be 1/20 and 1 m, respectively. At the initial stage, a small random perturbation with an amplitude of $\Delta Z = 0.5$ m was added to the slope. The calculation domain was a rectangle of 4 km length and 1.2 km width, and a periodic boundary condition was set at both ends. h_c, the equilibrium slope, and the repose slope were assumed to be 4 m, 1/20, and 1/2, respectively. The calculation of the wave field was carried out every 10 steps in the calculation of beach changes. The detailed conditions for the calculation of development of sand spits and cuspate forelands with rhythmic shapes are summarized in **Table 2**.

3.2 Calculation results

3.2.1 Oblique wave incidence at an angle of 60°

Figures 11 and **12** show the calculation results of the development of sand spits from infinitesimal perturbation and the bird's eye view of the same results.

Calculation method	Type 4 BG model
Wave conditions	Incident waves: H_i = 1 m, T = 4 s, and wave direction θ_I = 60° relative to direction normal to initial shoreline
Berm height	h_R = 1 m
Depth of closure	h_c = 4 m (still water depth)
Equilibrium slope	$\tan\beta_c$ = 1/20
Angle of repose slope	$\tan\phi$ = 1/2
Coefficients of sand transport	Coefficient of longshore sand transport K_s = 0.2 Coefficient of Ozasa and Brampton term [12] K_2 = 1.62K_s Coefficient of cross-shore sand transport K_n = K_s
Mesh size	Δx = Δy = 20 m
Time intervals	Δt = 0.5 h
Duration of calculation	2.75×10^4 h (5.5×10^4 steps)
Boundary conditions	Shoreward and landward ends, q_x = 0; right and left boundaries, periodic boundary
Calculation of wave field	Energy balance equation [13] • Term of wave dissipation due to wave breaking: Dally et al. [14] model • Wave spectrum of incident waves: directional wave spectrum density in Goda [15] • Total number of frequency components N_F = 1 and number of directional subdivisions N_θ = 8 • Directional spreading parameter S_{max} = 25 • Coefficient of wave breaking K = 0.17 and Γ = 0.3 • Imaginary depth between depth h_0 (0.5 m) and berm height h_R • Wave energy = 0 where $Z \geq h_R$ • Lower limit of h in terms of wave decay due to wave breaking, 0.5 m

Table 2.
Conditions for calculation of development of sand spits and cuspate forelands with rhythmic shapes.

The small perturbation applied to the slope at the initial stage developed into 11 cuspate forelands within 5×10^3 steps (**Figures 11(b)** and **12(b)**), and the shoreline projection increased with time together with the rightward movement. Because of the periodic boundary condition at both ends, the cuspate forelands that moved away through the right boundary reentered the calculation domain through the left boundary [4, 5]. After 10^4 steps, the shoreline protrusion increased and developed as slender sand spits (**Figures 11(c)** and **12(c)**). After 2×10^4 steps, the small-scale sand spits located adjacent to each other had merged into large-scale sand spits and disappeared, resulting in the formation of six sand spits (**Figures 11(d)** and **12(c)**).

Two reasons for the above changes are considered [1, 2, 4, 5]. (1) Of the two sand spits of different scales, the small sand spits move faster than the large ones in the absence of the wave-sheltering effect, and then the small sand spits catch up and merge with the large ones. (2) On the lee of sand spits with an elongated neck, a wave-shelter zone is formed, and the velocity of the small sand spits is reduced in the zone because of low wave energy, resulting in the stoppage of the movement of the sand spits and in the merging of small sand spits with larger spits. Furthermore, the sand spits developed and protruded, because (1) their tip is semicircular, meaning that the angle between the direction normal to the shoreline
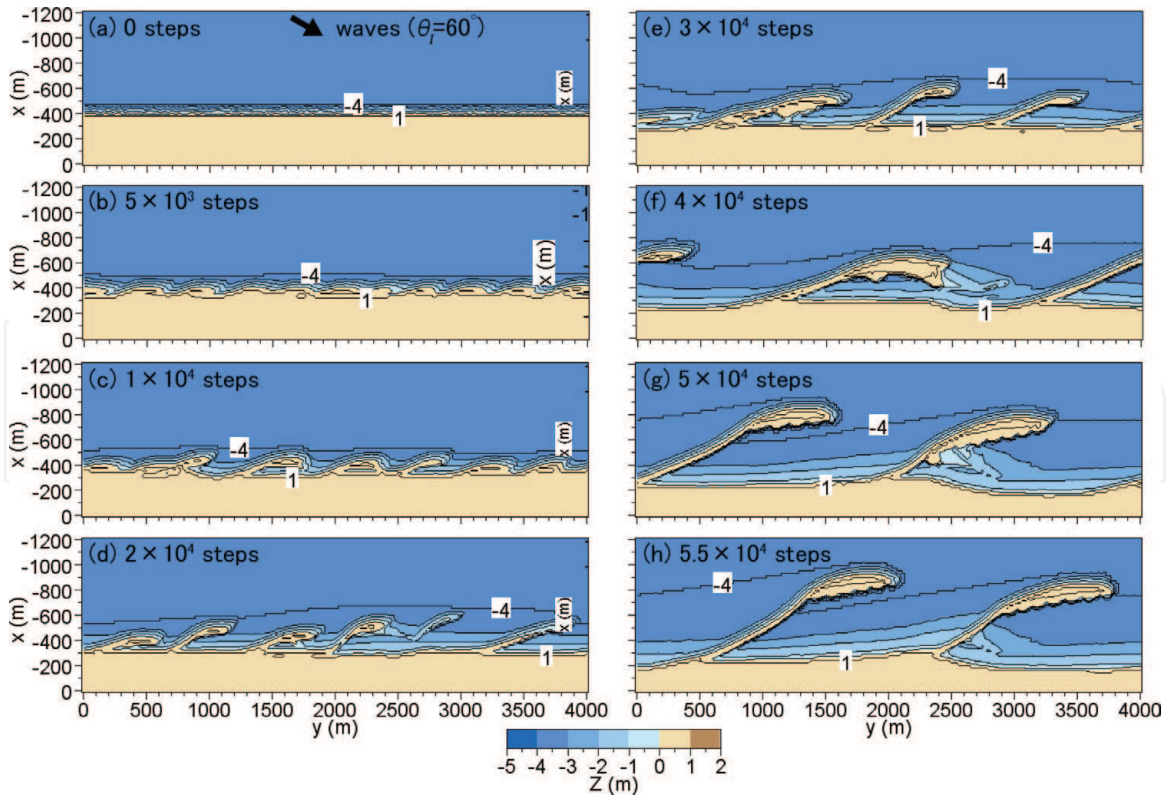
Figure 11.
Development of sand spits from infinitesimal perturbation when waves are obliquely incident at an angle of 60° [4, 5].

and the wave direction exceeds 45° at a point along the shoreline, and the shoreline protrusion occurs at such a point owing to high-angle wave instability. (2) In a wave-shelter zone, sand transport is significantly reduced, whereas it is enhanced near the tip of the sand spits, and thus, the derivative of the sand transport rate takes a maximum value near the boundary between the tip of the sand spits and the wave-shelter zone, inducing the protrusion of sand spits.

After 3×10^4 steps, the small sand spits located in the wave-shelter zone of the large-scale sand spits had stopped moving and merged into the large-scale sand spits, resulting in a decrease in the number of sand spits (**Figures 11(e)** and **12(e)**). After 4×10^4 steps, the number of sand spits decreased to two, and the tip of the sand spits approached close to the original shoreline, permitting the downcoast passage of the sand (**Figure 11(f)**). Two large-scale sand spits were formed up to 5×10^4 steps, and the offshore contour of −4 m depth obliquely extended toward the tip of the sand spit (**Figures 11(g)** and **12(f)**). These features are in good agreement with those measured around sand spits in lakes and bays [16].

3.2.2 Oblique wave incidence at angles of ±60° with probability of 0.50:0.50

When waves were obliquely incident at angles of ±60° with probability of 0.50:0.50, triangular cuspate forelands had developed after 10^4 steps (**Figures 13** and **14**). In this case, symmetric cuspate forelands were formed, and small-scale cuspate forelands disappeared and merged with larger cuspate forelands [4, 5]. Because of the same probability of the occurrence of both wave directions, no net longshore sand transport and no unidirectional movement of the sand body occurred. After 2×10^4 steps, the number of triangular cuspate forelands had been reduced to five (**Figures 13(d)** and **14(c)**), and they further continued to develop with the merging of small-scale cuspate forelands. After 4×10^4 steps, four symmetric cuspate forelands had developed (**Figures 13(f)** and **14(e)**).
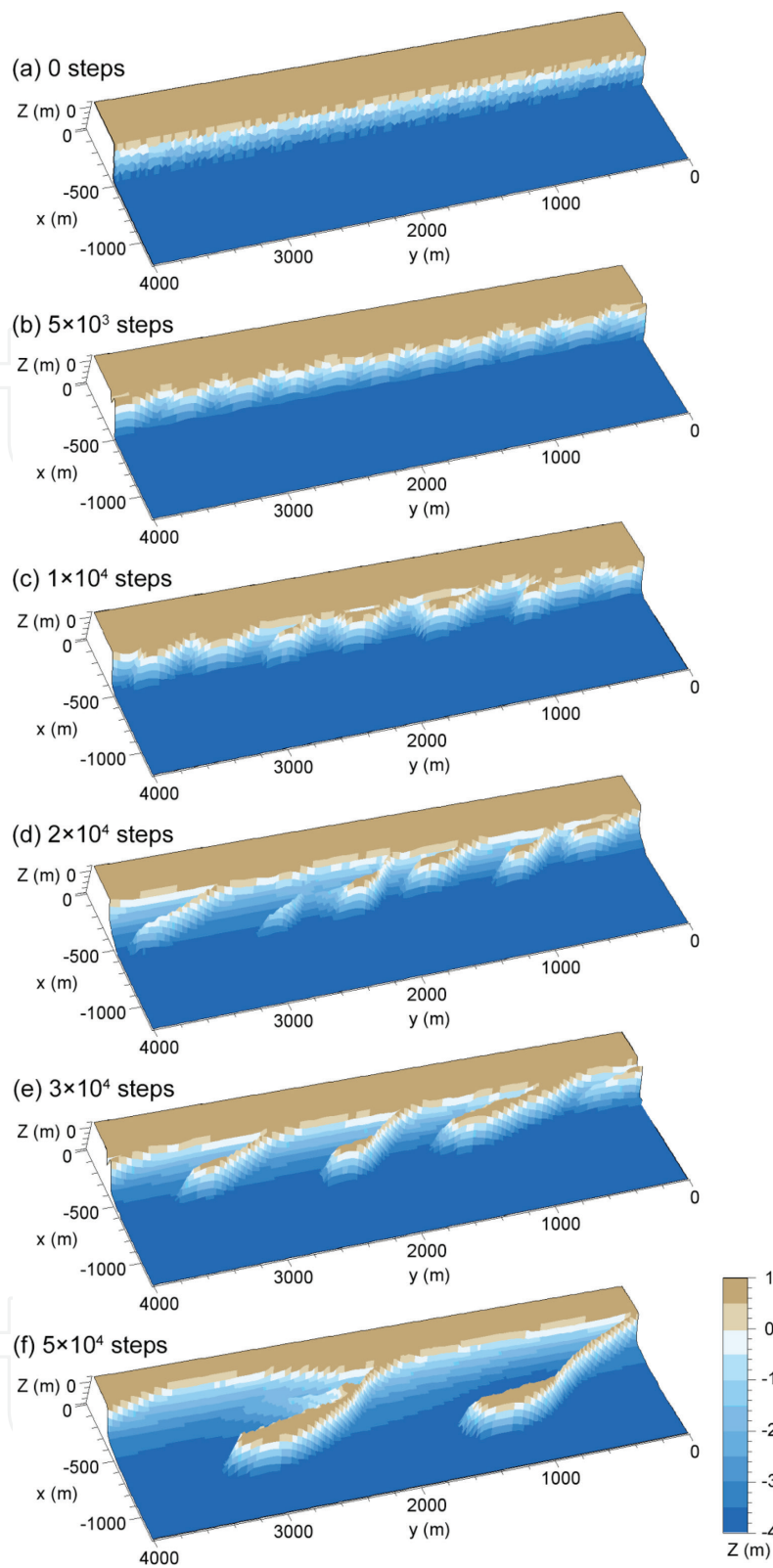
Figure 12.
Bird's eye view of the development of sand spits.

3.2.3 Oblique wave incidence at angles of ±60° with different probabilities

Waves were obliquely incident at angles of ±60°, and the probability of occurrence of waves was changed as 0.60:0.40, 0.65:0.35, 0.70:0.30, 0.75:0.25, and 0.80:0.20, i.e., the condition that rightward longshore sand transport gradually increased with the change in probability.

In case with probability of 0.60:0.40, symmetric cuspate forelands that slightly inclined rightward have developed (**Figure 15**) [5]. Because of the rightward net
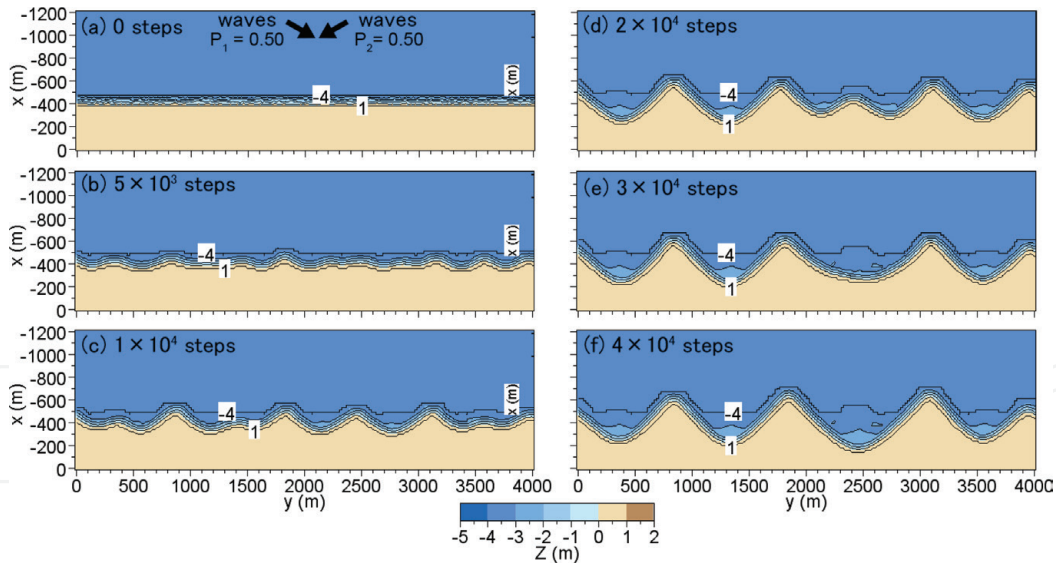
Figure 13.
Formation of cuspate forelands when waves were obliquely incident at angles of ±60° with probability of 0.50:0.50 [4, 5].

longshore sand transport, cuspate forelands developed while moving rightward. The shoreline left of the tips of cuspate forelands extended straight, whereas the shoreline curvature increased immediately right of the tips, forming a hooked shoreline. The contour of 4 m depth extended toward the tips of the forelands while obliquely intersecting with the shoreline left of the tip of the foreland, and then it extended parallel to the shoreline from the tip of the foreland with a large curvature.

In case with probability of 0.65:0.35, the steepness of the cuspate forelands increased after 2×10^4 steps, and a hooked shoreline inclined rightward had formed, because the probability of occurrence of waves incident from the left increased (**Figure 16(a)**) [4, 5]. After 3×10^4 steps, sand spits were formed at the tips of the cuspate forelands (**Figure 16(b)**), and a shallow bay was formed between the apexes, and sand spits obliquely extended rightward from the tips of the cuspate forelands with a larger angle than that in **Figure 13** until 4×10^4 steps (**Figure 16(c)**). In particular, the calculation results obtained after 4×10^4 steps and the case in a lagoon facing the Chukchi Sea shown in **Figure 1** are in good agreement.

In case with probability of 0.70:0.30, sand spits had already developed after 2×10^4 steps (**Figure 17(a)**), and these sand spits further elongated downcoast after 3×10^4 steps (**Figure 17(b)**), and sand spits with a narrow neck at the connecting point to the land and a long head were formed until 4×10^4 steps (**Figure 17(c)**) [5]. The number of sand spits reduced to two from four in the case with probability of 0.70:0.30. Similarly, in case with probability of 0.75:0.25, a slender sand spit started to develop after 2×10^4 steps (**Figure 18(a)**), and the sand spit with a narrow neck had elongated rightward after 3×10^4 steps (**Figure 18(b)**). After 4×10^4 steps, sand spits with a long, slender neck had developed (**Figure 18(c)**). Although contours shallower than 3 m depth extended parallel to the shoreline, while forming the main body of the sand spits, the contour of 4 m depth had an embayment downcoast of the sand spits [5]. Finally, in the case for probability of 0.80:0.20, many sand spits with a head extending in parallel with the original shoreline were formed close to the coastline after 2×10^4 steps, because the probability of occurrence of waves from the left markedly increased (**Figure 19(a)**). After 3×10^4 steps, the lengths of sand spits had further increased, but the head of sand spits extended parallel to the coastline similar to the development of longshore sand bars (**Figure 19(b)**).
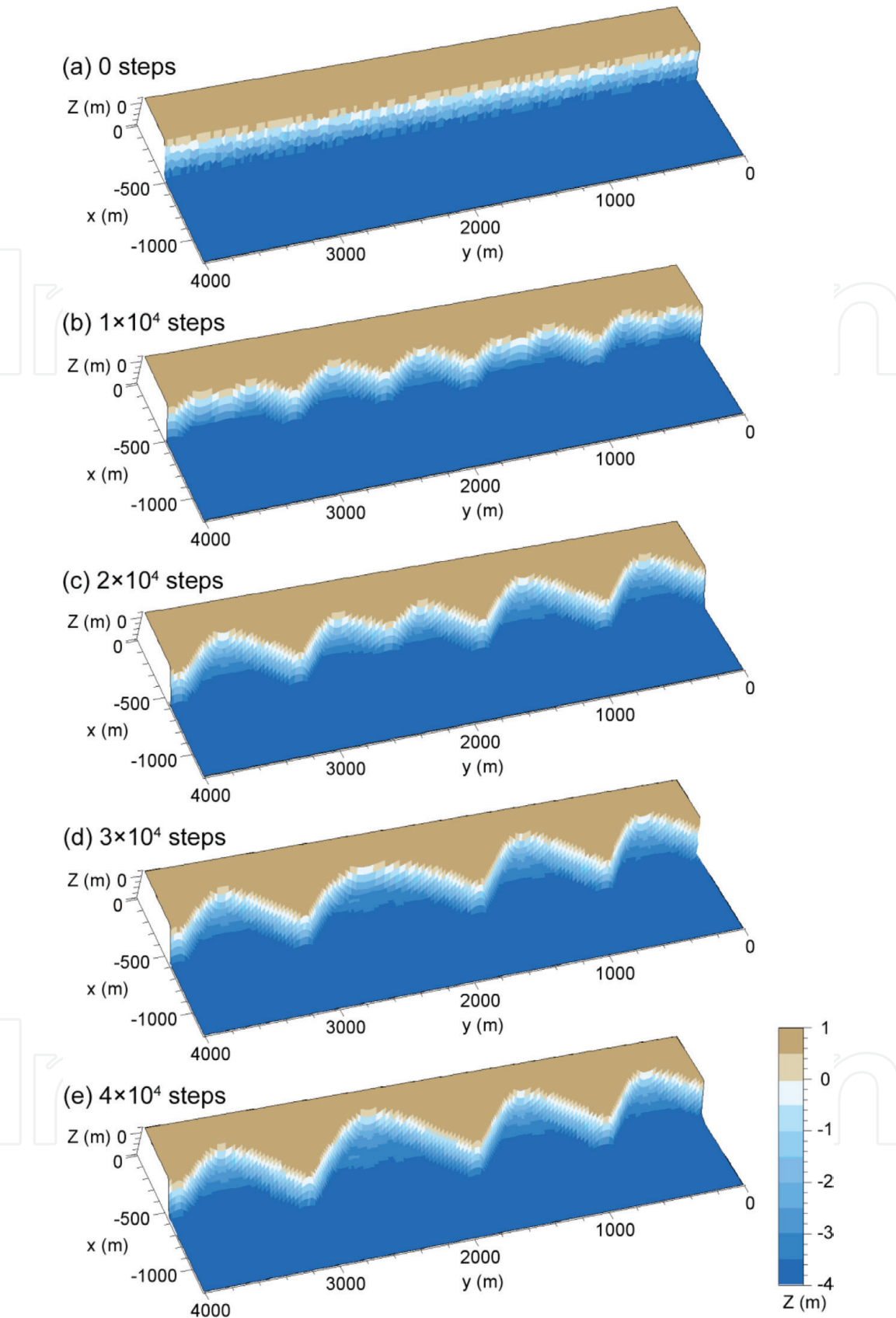
Figure 14.
Bird's eye view of the development of cuspate forelands.

Thus, symmetric cuspate forelands were formed when waves were obliquely incident at angles of ±60° with an equivalent probability of the occurrence of waves. With probability of 0.60:0.40, the asymmetry of cuspate forelands increased, and sand spits started to form after 2×10^4 steps with a probability of 0.65:0.35.
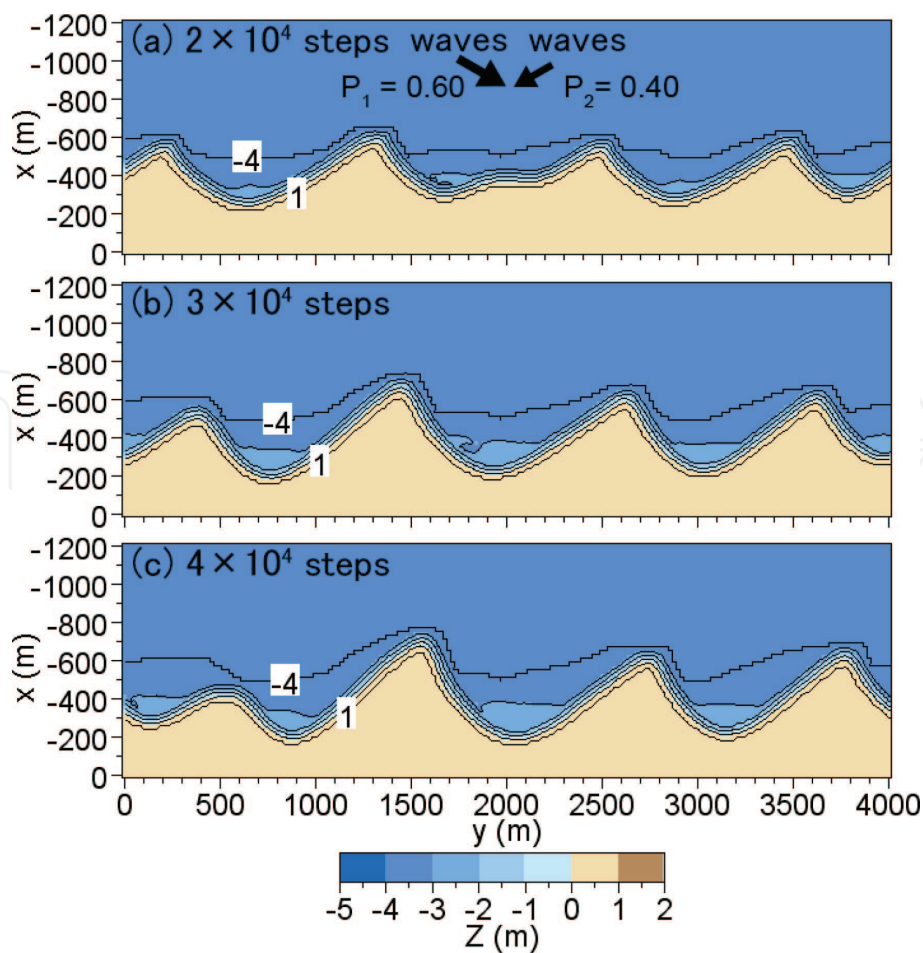
Figure 15.
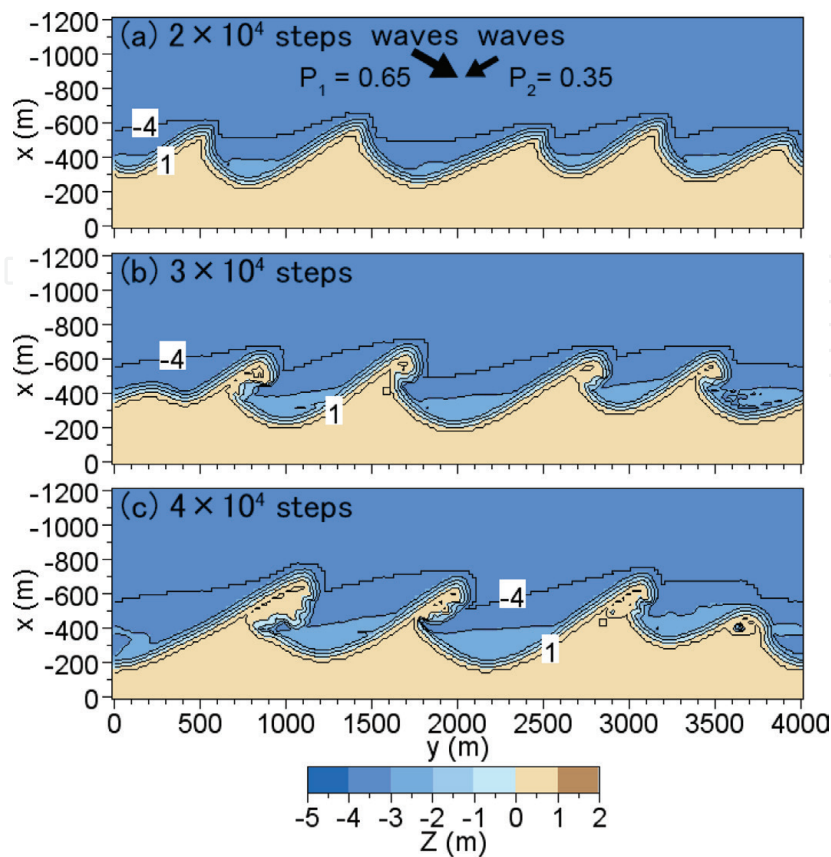*Formation of cuspate forelands when waves were obliquely incident at angles of ±60° with probability of 0.60:0.40 [5].*

Figure 16.
Formation of cuspate forelands when waves were obliquely incident at angles of ±60° with probability of 0.65:0.35 [4, 5].
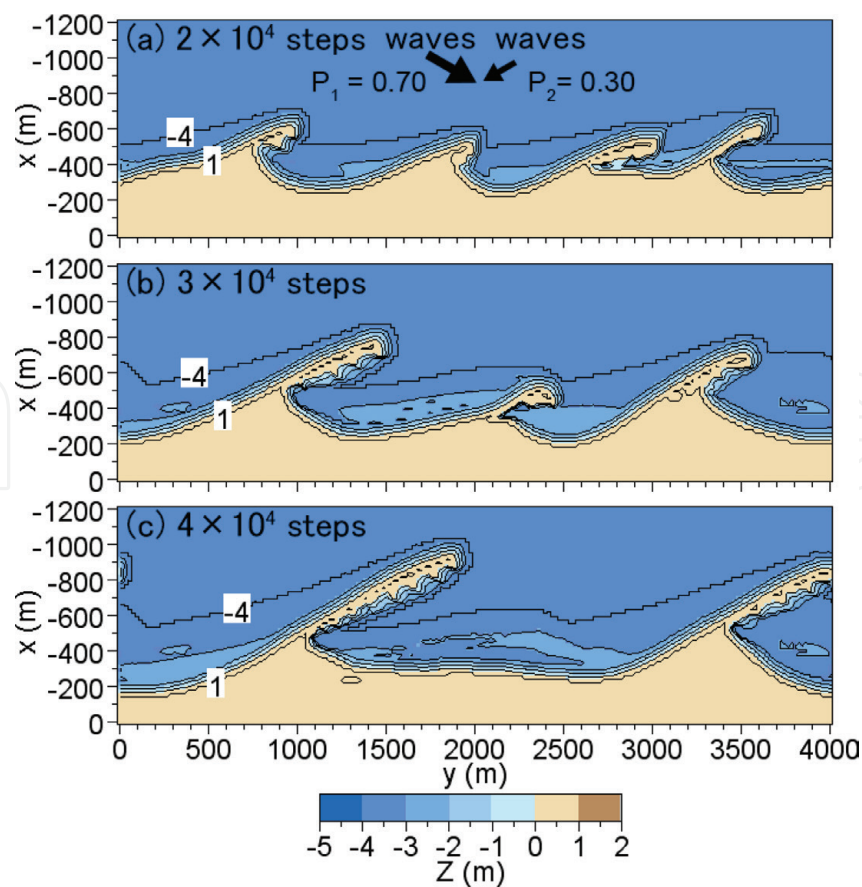
Figure 17.
Formation of cuspate forelands when waves were obliquely incident at angles of ±60° with probability of 0.70:0.30 [5].
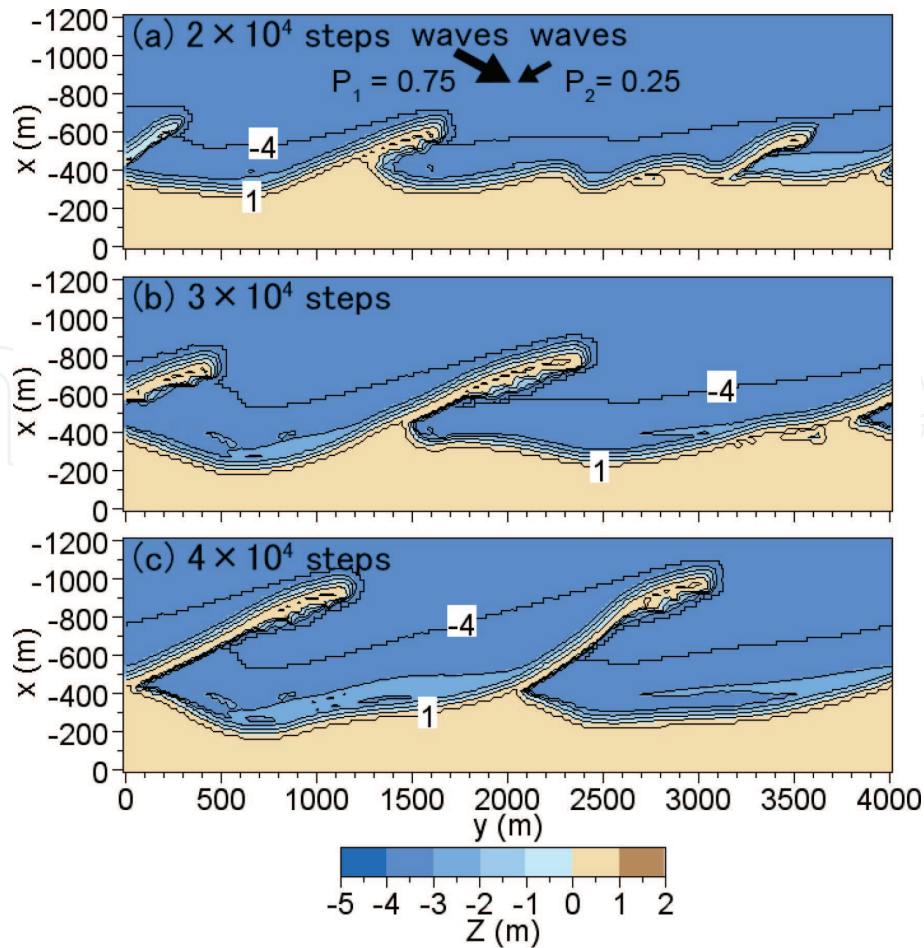

Figure 18.
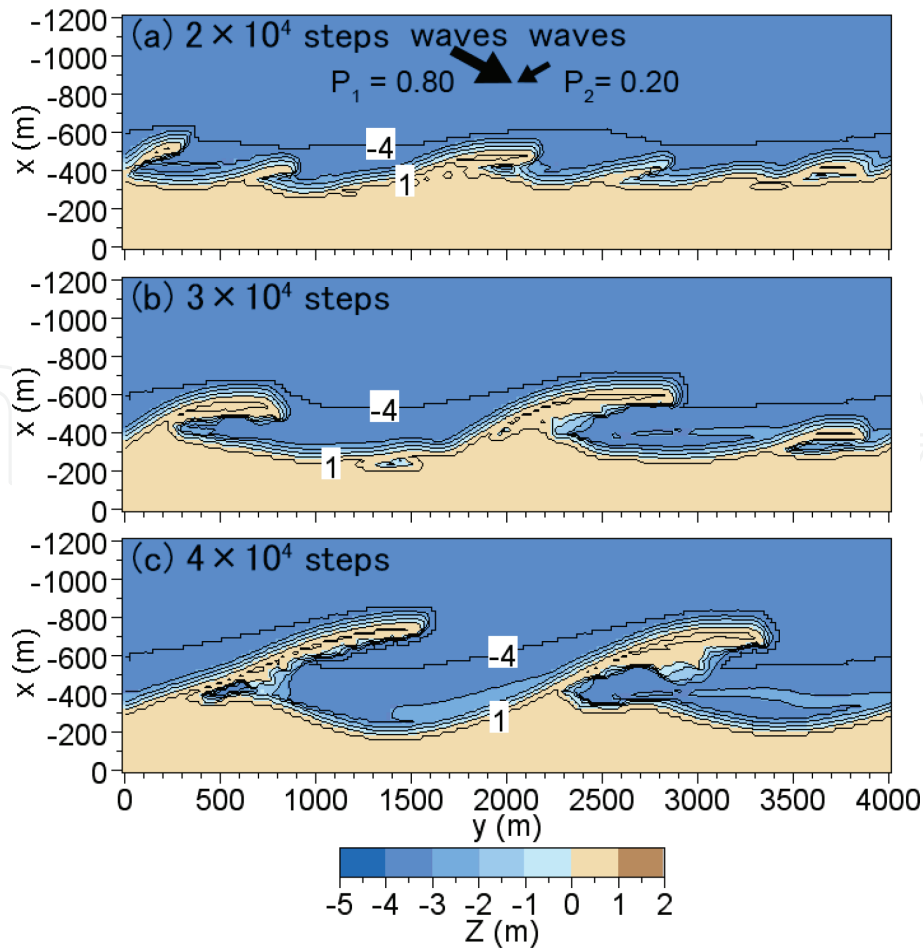*Formation of cuspate forelands when waves were obliquely incident at angles of ±60° with probability of 0.75:0.25 [5].*

Figure 19.
Formation of cuspate forelands when waves were obliquely incident at angles of ±60° with probability of 0.80:0.20 [5].

Increasing probabilities of occurrence of waves from the left, sand spits with a head extending parallel to the original shoreline developed [5]. In all cases of the development of sand spits, a narrow neck was formed at the connecting point to the land, a general characteristic of the topography around a sand spit [1]. Thus, the mechanism based on the high-angle wave instability and the evolution of 3-D beach changes was explained well by the Type 4 BG model. Although the size of the sand spits formed along the north shore of the Azov Sea is much larger than that of the calculation results, the geometrical configurations of the calculated results are in good agreement with the measured results. Sand spits A, B, C, and D (**Figure 1**) have been formed mainly by waves obliquely incident from the east. The sand spit D located at the west end has a long, slender neck; this feature is in good agreement with the calculation results of the sand spit formed under the incidence of unidirectional waves (**Figure 11(h)**). In addition, the width and length of the neck of the sand spit become thick and short in the order of sand spits C, B, and A, along with the development of a hooked shoreline behind each sand spit. These conditions are very similar to those for the development of sand spits when waves were incident from two directions with different probabilities.

The shape of the sand spit A is very similar to that of the sand spit second from the right end in **Figure 16(c)** calculated with probability of 0.65:0.35, and that of the sand spit C is similar to that located at right end in **Figure 17(b)** calculated with probability of 0.70:0.30 [5]. On the north shore of the Azov Sea, an easterly wind is considered to be predominant, and sand spit D located at the west end could receive sufficiently large wave energy from the east because of a long fetch distance, whereas the wave action from the west is weak because of short fetch distance. As a result, wave action from the

east became stronger, and the sand spit with a narrow, slender neck was considered to be formed. In contrast, for the sand spit A, the fetch distance from the east was so short that the wave action from the east was weakened, whereas wave action from the west was strengthened because of a long fetch distance. In addition, the increase in the fetch distance of the easterly wind was considered to cause the increase in the scale of the sand spit. Here, the development of sand spits and cuspate forelands with rhythmic shapes was predicted, when waves were obliquely incident at large angles relative to the direction normal to the shoreline. Similarly, the effects of anthropogenic factors on development of sand spits and cuspate forelands with rhythmic shapes can be predicted using Type 4 BG model, as described in [5]. Moreover, the Type 4 BG model can be applied to predict the interaction and merging of cuspate forelands formed at the end of multiple sandy islands under the condition that waves are incident from two completely opposite directions [17] and the shoreline variation at tip of cuspate foreland in response to change in wave direction when waves are cyclically incident from two completely opposite directions [18]. The formation of recurved sand spit when waves are cyclically incident from two different directions can be also predicted [19].

4. Conclusions

In Chapter 7, two topics were discussed and topographic changes were predicted using the Type 4 BG model: (1) formation of a cuspate foreland and (2) development of sand spits and cuspate forelands with rhythmic shapes.

1. The morphology of the cuspate foreland located at the northeast end of Graham Island and the cuspate forelands formed at the tip of Hon Bip Island was investigated, and the Type 4 BG model was used to predict the development of a cuspate foreland for waves incident from two opposite directions. It was concluded that not only the cuspate foreland with a sharp tip was formed but also a closed water body remained near the tip of the foreland.

2. The development of sand spits and cuspate forelands with rhythmic shapes was predicted using the Type 4 BG model. A single sand spit elongated when a single wave direction from the $-x$-axis was assumed, whereas a symmetric cuspate foreland was formed when waves with the same probabilities were incident from two opposite directions, and an asymmetric cuspate foreland was formed with different probabilities. Zenkovich [1] qualitatively explained these features using a schematic diagram, but here, these features observed in the field were successfully explained using the BG model.

Author details

Takaaki Uda[1*], Masumi Serizawa[2] and Shiho Miyahara[2]

1 Public Works Research Center, Tokyo, Japan

2 Coastal Engineering Laboratory Co., Ltd., Tokyo, Japan

*Address all correspondence to: uda@pwrc.or.jp

IntechOpen

References

[1] Zenkovich VP. Processes of Coastal Development. New York: Interscience Publishers, Div. of John Wiley and Sons, Inc; 1967. p. 751

[2] Ashton A, Murray AB, Arnault O. Formation of coastline features by large-scale instabilities induced by high angle waves. Nature. 2001;**414**:296-300

[3] Ashton A, Murray AB. High-angle wave instability and emergent shoreline shapes: 1. Modeling of sand waves, flying spits, and capes. Journal of Geophysical Research. 2006;**111**:F04011. DOI: 10.1029/2005JF000422

[4] Serizawa M, Uda T, Miyahara S. Prediction of development of sand spits and cuspate forelands with rhythmic shapes caused by shoreline instability using BG model. In: Proc. 33rd ICCE, sediment. 35. 2012. pp. 1-11. http://journals.tdl.org/icce/index.php/icce/article/view/6534/pdf_534

[5] Uda T, Serizawa M, Miyahara S. Development of sand spits and cuspate forelands with rhythmic shapes and their deformation by effects of construction of coastal structures (Chap. 19). In: Awrejcewicz J, editor. Computational and Numerical Simulations. Rijeka: InTech; 2014. pp. 419-450. http://www.intechopen.com/books/computational-and-numerical-simulations/development-of-sand-spits-and-cuspate-forelands-with-rhythmic-shapes-and-their-deformation-by-effect#article-front

[6] Serizawa M, Uda T, Miyahara S. Model for predicting formation of a cuspate foreland. In: Coastal Sediments'15, CD-Rom No. 65. 2015. pp. 1-14

[7] Littlewood R, Murray AB, Ashton AD. An alternative explanation for the shape of 'log-spiral' bays. In: Coastal Sediments'07. 2007. pp. 341-350

[8] van den Berg N, Falqués A, Ribasz F. Long-term evolution of nourished beaches under high angle wave conditions. Journal of Marine Systems. 2011;**88**(1):102-112

[9] Scheffers AM, Scheffers SR, Kelletat DH. The coastlines of the World with Google Earth. In: Coastal Research Library. Vol. 2. New York: Springer; 2012. p. 293

[10] Uda T, Serizawa M, Miyahara S. Formation of cuspate foreland in field subject to wave-sheltering effect of islands. In: Proc. 35th Conf. Coastal Eng., sediment. 4. 2016. pp. 1-14. https://icce-ojs-tamu.tdl.org/icce/index.php/icce/article/view/8102/pdf

[11] Miyahara S, Uda T, Serizawa M. Prediction of formation of land-tied islands. In: Proc. 34th ICCE. 2014. pp. 1-14. https://journals.tdl.org/icce/index.php/icce/article/view/7108/pdf_412

[12] Ozasa H, Brampton AH. Model for predicting the shoreline evolution of beaches backed by seawalls. Coastal Engineering. 1980;**4**:47-64

[13] Mase H. Multidirectional random wave transformation model based on energy balance equation. Coastal Engineering Journal, JSCE. 2001;**43**(4):317-337

[14] Dally WR, Dean RG, Dalrymple RA. A model for breaker decay on beaches. In: Proc. 19th ICCE. 1984. pp. 82-97. https://journals.tdl.org/icce/index.php/icce/article/view/3787/3470

[15] Goda Y. Random Seas and Design of Maritime Structures. Tokyo: University of Tokyo Press; 1985. 323 p

[16] Uda T, Yamamoto K. Beach erosion around a sand spit—an example of Mihono-Matsubara sand spit. In: Proc. 24th ICCE. 1994. pp. 2726-2740. https://journals.tdl.org/icce/index.php/icce/article/view/5141/4819

[17] Miyahara S, Uda T, Serizawa M. Interaction and mergence of cuspate forelands formed at end of multiple sandy islands under waves. In: Proc. 36th Conf. Coastal Eng. 2018. In press

[18] Miyahara S, Uda T, Serizawa M. Shoreline variation at tip of cuspate foreland in response to change in wave direction. In: Proc. 9th Int. Conf. on Asian and Pacific Coasts (APAC2017). 2017. pp. 455-466

[19] Serizawa M, Uda T, Miyahara S. Prediction of formation of recurved sand spit using BG model. In: Proc. 36th Conf. Coastal Eng. 2018. In press